River Flow 2010 - Dittrich, Koll, Aberle & Geisenhainer (eds) - © 2010 Bundesanstalt für Wasserbau ISBN 978-3-939230-00-7

Effects produced by breach morphology on the outflow discharge due to the overtopping of earthfill dams

G. De Lorenzo & F. Macchione
LAMPIT (Laboratorio di Modellistica Numerica per la Protezione Idraulica del Territorio); Dipartimento di Difesa del Suolo – University of Calabria, Via P. Bucci, 42/b; 87036 Rende (CS), Italy.

ABSTRACT: Many recent studies have pointed out that further improvements in dam breach modelling are still necessary, in particular about the description of the breach enlargement mechanisms. Among these, a correct description of the breach morphology plays an important role on the discharge hydrograph flowing out from the breach. In this paper, the sensitivity analysis of a physically based dam breach model to the breach morphology is shown. The model was proposed by Macchione and it is specifically intended to be used for the breaching of earthfill dams. The model needs only one calibration parameter whose value was obtained on the basis of 12 dam breach event simulations concerning uniformly erodible earthfill dams. This paper concerns the effects on the peak discharge and on the outflow hydrograph produced by the morphology of the breach and in particular by the value of the breach side slope. The analysis has been carried out for breaching caused by overtopping.

Keywords: Dams, Dam failure, Earthfill, Peak flow, Flash floods

1 INTRODUCTION

The ability of dam breach numerical models to give reliable results about the outflow hydrograph lies on a correct description of the essential physical aspects of the phenomenon like hydraulics, breach morphology and widening process. In general the enlargement of the breach is produced by both continuous erosion and discrete breach sides collapses. Moreover the process is highly influenced by the soil used for the dam and in particular by its cohesive or non-cohesive nature (Powledge et al, 1989).

The aspects concerning the breach shape and the enlargement process have been widely investigated in the last years through physical modelling. Many laboratory and field tests have been carried out in the framework of IMPACT project, concerning mainly cohesive and non-cohesive dams. These tests seem to prove that during the enlargement of the breach, its sides, at least for the portion above the water level, are usually very steep or even near vertical (IMPACT, 2005). Similar results have been found, through some laboratory experiments, by Rozov (2003) which observed a rectangular breach.

Even more complex is the description of the overall phenomenon of breach formation and enlargement. A detailed description of breaching process, among non-cohesive soils, was given by Coleman and Andrews (2000). Hanson et al. (2005) and Hunt et al. (2005), through some field tests, provided an accurate description of the headcut formation and advance and of the breach enlargement for cohesive dams. They also remarked that these processes are strongly influenced by the geotechnical properties of the dam material. In particular, even small variations in some properties like particle size, or water content, can produce great variations to the erosion strength and therefore in the discharge from the breach.

The previous observations suggest that the research in dam breach modelling encompasses various aspects and it needs more time for their development (Morris et al., 2008). Meanwhile the researchers also have to meet the needs of practical engineering with reliable methods that allow to compute the peak discharge or the flood hydrograph caused by the erosion of earthen dams.

A comprehensive review of dam breach modelling can be found in Singh (1996). Recently Macchione (2008) proposed a dam breach model with a simplified approach. The model considers a triangular breach cross section until the lower vertex reaches the natural ground, then the breach becomes trapezoidal and erosion occurs only along the breach sides. The model also considers the breach as a throat through which it is reasonable to assume the occurrence of critical flow (Macchione, 1986). The amount of eroded volume is computed as a function of shear stress along breach sides. The slope of breach sides is fixed a priori and it is constant throughout the erosion process. Moreover the model needs only one calibration parameter for the closure of the erosion law.

The most interesting feature of this model is that, with a single value of the calibration parameter, very good results have been obtained for the simulation of 12 historical dam breach events with observed peak discharges covering 3 orders of magnitude.

These results suggest that the model can simulate the flood hydrograph of a dam breach event with a synthetic approach, so without the need of an explicit description of many aspects (like breach side collapses or headcut migration) that actually are very complex. The model takes into account these aspects within a simplified erosion law that describes the enlargement of the breach as a function of shear stresses and with a calibration parameter.

A limitation of the model is that the value of breach side slope needs to be assumed a priori so that a sensitivity analysis was carried out by Macchione and Rino (2008) to provide a guidance on a value to choose for tanβ for prediction. The above sensitivity analysis shown that for small reservoirs the highest values of peak discharge are obtained assuming tanβ=0.2, whereas for large reservoirs the highest values of peak discharge are obtained assuming tanβ=2. The present paper focuses one's attention on intermediate values of tanβ, within the range 0.2÷2 in order to highlight the role of breach morphology in dam breach modelling.

2 MODEL EQUATIONS

In order to carry out a sensitivity analysis, Macchione and Rino (2008) rewrite the equations of the model in terms of the following dimensionless variables:

$$h_c^* = \frac{h_c}{Z_M}; \quad Z^* = \frac{Z}{Z_M}; \; Y^* = \frac{Y}{Z_M}; \; t^* = t\frac{v_e}{Z_M};$$

$$Q^* = \frac{Q}{g^{1/2} Z_M^{5/2}}; \; w_c^* = \frac{w_c}{Z_M};$$

in which h_c is the critical depth, Z is the surface level in the reservoir, Y is the vertical distance between the vertex of the triangular breach and the natural ground, Q is the discharge from the breach, w_c is the embankment crest width, Z_M is the height of the dam, t is the time and v_e is a characteristic velocity that affects the erosion velocity dY/dt. The value of v_e was obtained through model calibration (Macchione, 2008).

The following equations were obtained:

$$\frac{dY^*}{dt^*} = -\frac{1}{2}\left(\frac{4}{5}\right)^2 \frac{(\sin\beta)^{-\frac{3}{2}}\left(Z^* - Y^*\right)^2}{\left(1-Y^*\right)\left[\left(1-Y^*\right)\frac{s_u + s_d}{2} + w_c^*\right]} \quad (1)$$

$$\frac{dZ^*}{dt^*} = -2^{-1/2}\left(\frac{4}{5}\right)^{\frac{5}{2}} \frac{Z^{*(1-\alpha_0)}}{\alpha_0 G}\left(Z^* - Y^*\right)^{\frac{5}{2}} \tan\beta \quad (2)$$

$$\frac{dY^*}{dt^*} = -\frac{\left(h_c^* - Y^*\right)^{-\frac{3}{2}}\left(h_c^* - 2Y^*\right)h_c^{*2}}{2\sin\beta\left(\frac{s_u + s_d}{2} + w_c^*\right)}\left(\frac{h_c^*}{\sin\beta} - Y^*\right)^{\frac{1}{2}} \quad (3)$$

$$\frac{dZ^*}{dt^*} = -2^{-1/2}\frac{Z^{*(1-\alpha_0)}}{\alpha_0 G}\frac{\left(h_c^* - 2Y^*\right)^{3/2}}{\left(h_c^* - Y^*\right)^{\frac{1}{2}}} h_c^{*\frac{3}{2}} \tan\beta \quad (4)$$

Equations (1) and (2) describe respectively the enlargement of the breach and the depletion of the reservoir during the triangular stage, whereas equations (3) and (4) are valid for the trapezoidal stage. The meaning of each variable can be deduced from fig.1, while a detailed explanation of the model can be found in Macchione (2008) and (Macchione and Rino, 2008).

The parameter G has the following expression

$$G = v_e \frac{W_M}{\sqrt{g} Z_M^{7/2}} \quad (5)$$

in which v_e is the calibration parameter, and W_M is the volume of stored water at Z_M. The stored volumes are given as a function of level Z by the reservoir volume curve:

$$W = W_0 Z^{\alpha_0}$$

so that $W_M = W_0 Z_M^{\alpha_0}$.

The parameter G therefore takes account of the sizes of the dam and of the reservoir. In particular,

high values of G are related to large reservoirs and indicate high erosion velocity in comparison with drainage velocity. Conversely, when the reservoir volume in small in relation to the dam height, G takes low values and the depletion of the reservoir is very fast. With reference to a value of 0.07 m/s for v_e, for the majority of real situations $0.01 \leq G \leq 1000$.

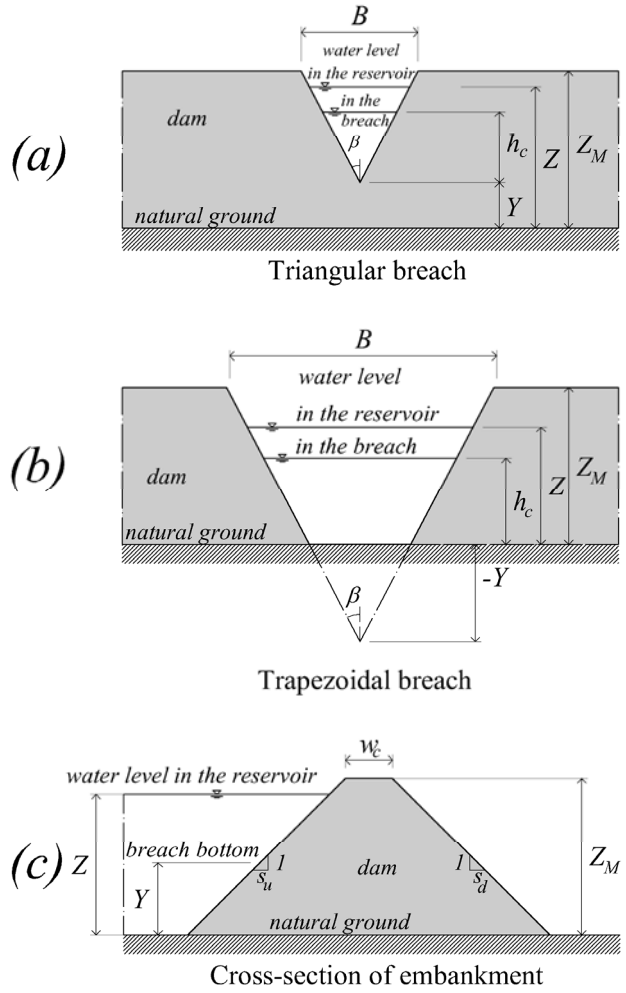

Figure 1: sketch of the dam and breach cross section.

3 EFFECT OF BREACH MORPHOLOGY

In the present study the variation of the breach side slope was explored within the range $0.2<\tan\beta<2$, as suggested by the frequency distribution of the final breach side slopes observed in dam breach events of the past (Macchione, 2008).

Plotting the values of the dimensionless peak discharge Q_p^* as a function of G shows that, in the range $5<G<15$, the value of Q_p^* does not vary significantly as $\tan\beta$ varies. For $G<5$, Q_p^* has a marked sensitivity to $\tan\beta$, and for values of $G>15$, sensitivity is more limited.

The plots shown in figure 2 report the discharge Q_p^* as a function of $\tan\beta$ for different values of G. In the plots the curves corresponding to $G=G^*$ are drawn; G^* is the value of G for which the value of Q_p^* obtained assuming $\tan\beta=0.2$ is equal to the value of Q_p^* obtained assuming $\tan\beta=2$. For values of $G>G^*$ the peak discharge increases with $\tan\beta$, otherwise for $G<G^*$ Q_p^* decreases as $\tan\beta$ increases. G^* varies as a function of the exponent α_0, as shown in Table 1.

Table 1: values of G^* as a function of α_0 (Macchione & Rino, 2008)

α_0	G^*
1	13
1.5	10
2	9
2.5	8
3	7
3.5	6.5
4	6

Moreover the areas of the plots are divided in two zones separated by a bold line. In the upper zone, which is marked by the letter A, the peak discharges happen when the breach is already in the trapezoidal shape, while in the lower portion, marked with letter B, the peak discharges happen when the breach is still triangular.

As an example, for $\alpha_0=4$, the peak discharge is reached when the breach is in the trapezoidal stage for any value of β only if G is greater than 2. Conversely for $G<0.02$, for any value of β, the cross section is still triangular when the peak discharge is reached. Therefore for $0.02 \leq G \leq 5$, the peak discharge happens during the triangular or the trapezoidal stage depending on the value chosen for β.

The influence of the parameter β on the shape of the flood hydrograph has been carried out assuming $\alpha_0=1 \div 4$. The results are shown for three different values of G: $G=G^*$, $G=10^{-1} \cdot G^*$ and $G=10 \cdot G^*$, since they summarise three representative scenarios of what has been previously said about the influence of β on the peak discharge.

Figure 3 shows the dimensionless flood hydrograph obtained for $G=10^{-1} \cdot G^*$ and how its shape changes with different values of $\tan\beta$. As already said the greatest value of the peak discharge is obtained for $\tan\beta=0.2$, and as a consequence the empting of the reservoir is faster. Moreover as greater values of $\tan\beta$ are assumed the empting of the reservoir becomes gradually slower, and the time to peak tend to remain unchanged.

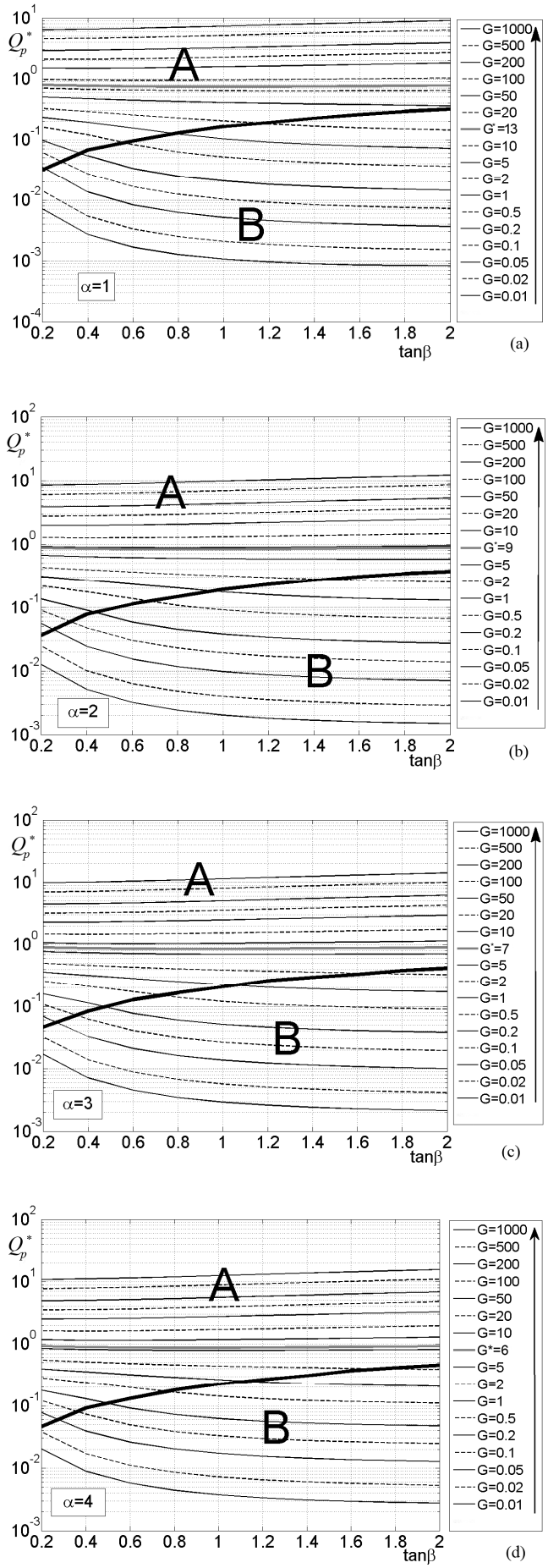

Figure 2: peak discharge as a function of β for α_0=1 (a), α_0=2 (b), α_0=3 (c), α_0=4 (d)

The figure 4 shows the temporal evolution of water level Z^* in the reservoir and of the elevation Y^* of the breach invert. For tanβ=0.2, Y^* decreases very fast and when the breach becomes trapezoidal the water level in the reservoir is still almost unchanged. In the other cases the drop of Y^* is slower and the water level (Z^*-Y^*) above the breach invert increases more slowly. For tanβ=2 the breach invert does not reach the natural ground and the breach remains triangular. The figure 5 shows the average width of the breach b_m^*, and so it also shows the breach growth since the area is proportional to b_m^*. The area of the breach grows faster for tanβ=0.2, but the maximum value is obtained for tanβ=2.

Figure 6 shows the dimensionless flood hydrograph obtained with G=G^*. The figure shows that the peak discharge is only slightly influenced by the value of the breach slope, and in particular the smallest values occur for values of tanβ placed in the middle of its range. Again the rising limb of the hydrograph is very faster only if the breach sides are very steep, and the influence on the time to peak and on the duration of the whole hydrograph tends to fade as tanβ is assumed higher. Figure 6, 7 and 8 show that the breach is always trapezoidal at the end of the process and that the peak discharge is obtained after the breach became trapezoidal and after the water level starts to drop.

The flood hydrograph shown in figure 9 is obtained assuming G=10·G^*. During the first stages of the breach enlargement, the water level keeps almost unchanged and the increase of critical depth in the breach lies only on the deepening of the breach invert. In this case the higher values of the peak discharge are obtained assuming tanβ=2. The figure also shows that the time to peak is generally poorly influenced by tanβ. Figure 9, 10 and 11 shows that also Z^* is poorly influenced by tanβ since the stored volume is so large that the water levels start to drop later than the breach becomes trapezoidal. The highest value of the peak discharge is thus obtained assuming tanβ=2 since it gives the higher values of the breach average width.

All the previous figures suggest that, apart from the value of G, the rising limb of the flood discharge is very steep if near vertical side slopes are assumed, and as a consequence the time to peak is anticipated. With low values of tanβ the discharge is higher during the first stages.

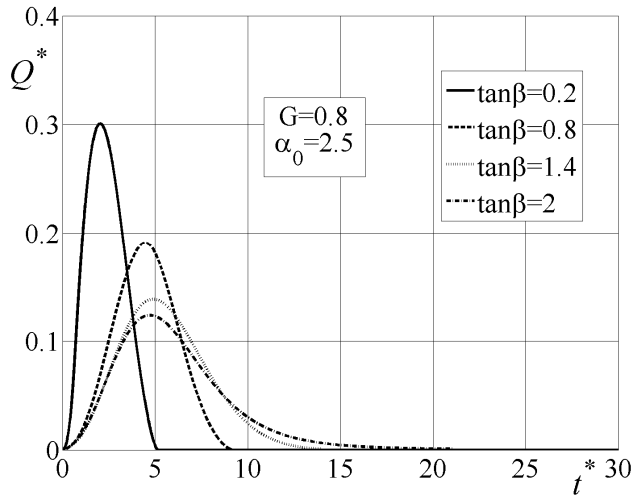

Figure 3: flood hydrograph for $G=10^{-1}G^*$

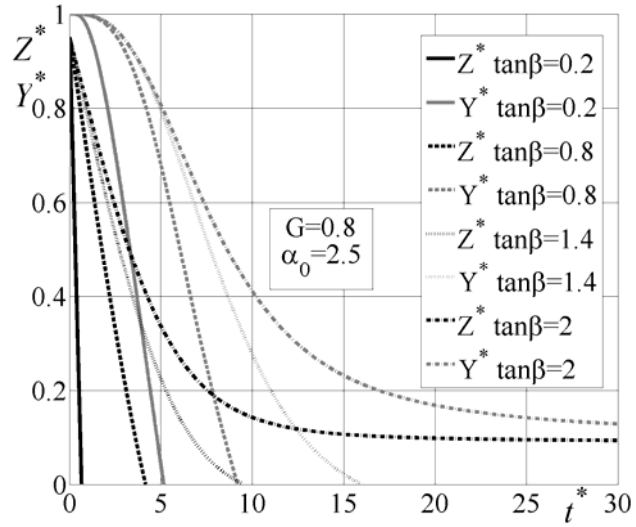

Figure 4: water depth and elevation of breach invert for $G=10^{-1}G^*$

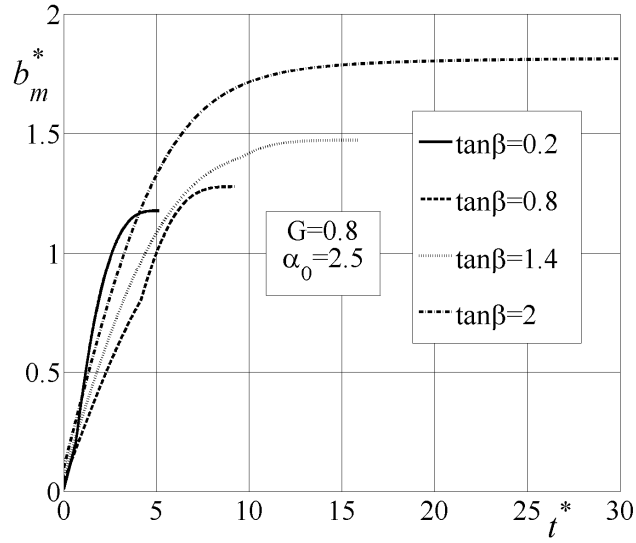

Figure 5: breach average width for $G=10^{-1}G^*$

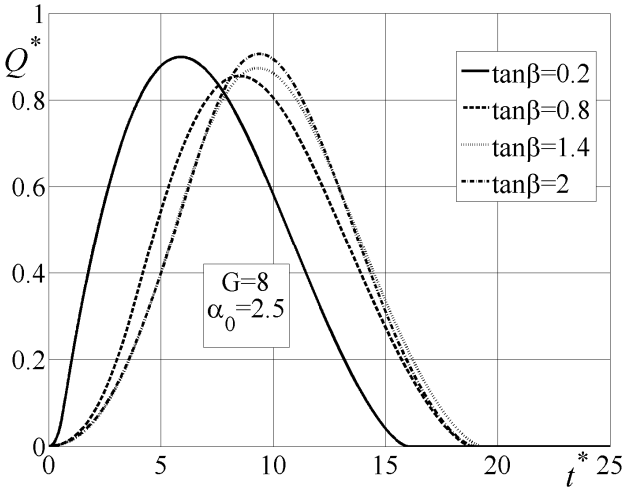

Figure 6: flood hydrograph for $G=G^*$

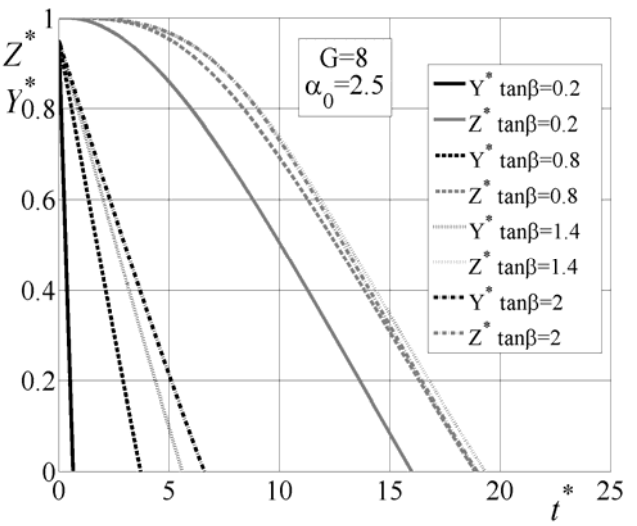

Figure 7: water level and elevation of breach invert for $G=G^*$

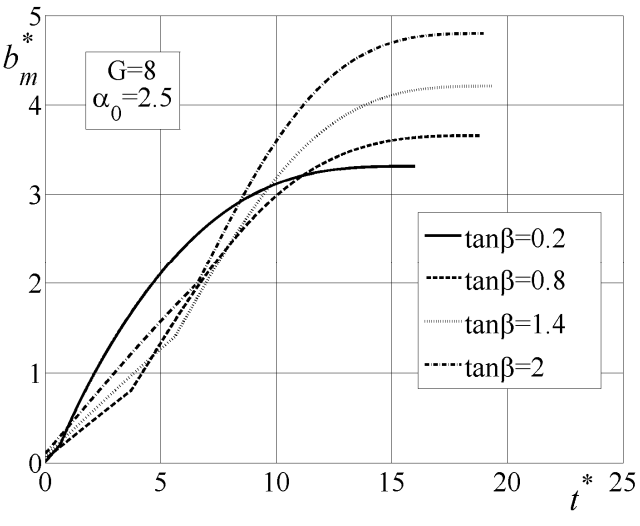

Figure 8: breach average width for $G=G^*$

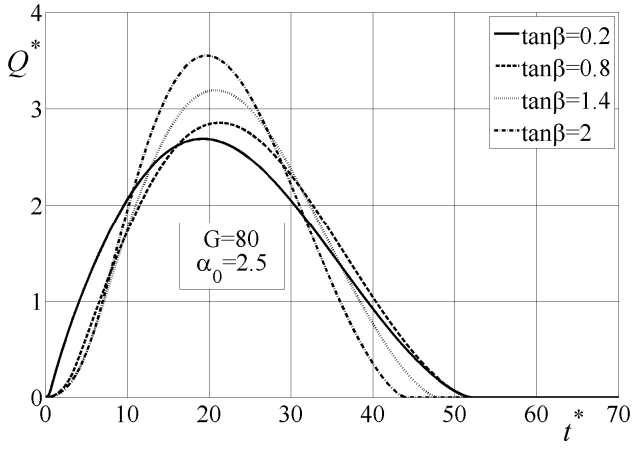

Figure 9: flood hydrograph for $G=10\cdot G^*$

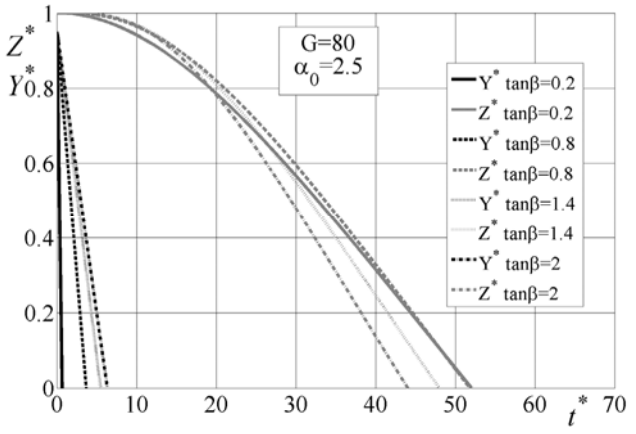

Figure 10: water level and elevation of breach invert for $G=10\cdot G^*$

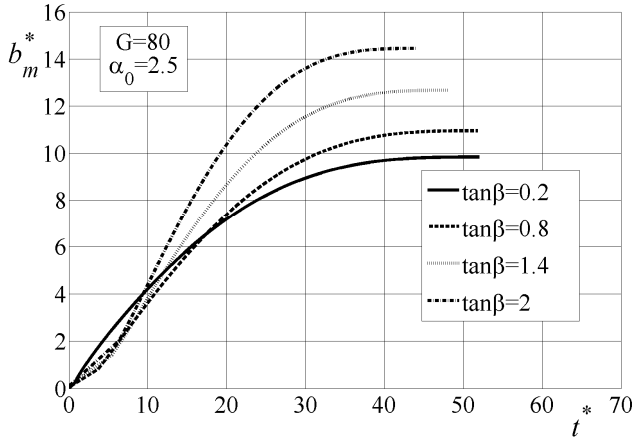

Figure 11: breach average width for $G=10\cdot G^*$

4 CONCLUSIONS

Breach morphology description is one of the most difficult problems in treating dam breach modeling. All the models proposed in literature have in some degree the same drawback in assuming the shape of the breach.

In the model analyzed here, on the basis of recorded historical observations of earthfill dam failures, a triangular shape and a trapezoidal shape for the breach have been assumed in the initial phase and for the subsequent phase of enlargement respectively. The values of peak discharges and, as a consequence, the shape of discharge hydrograph depend on the values assumed for tan β.

The analysis carried out in this paper shows that the values of peak discharge are greatly influenced by tanβ for $G<G^*$ and in the range $0.2\leq\tan\beta\leq1$. The greatest variations of time to peak are located in the same range of tanβ. For $G>G^*$ the influence of tanβ on peak discharges seems to be much more uniformly distributed on the whole range $0.2\leq\tan\beta\leq2$. For high values of G the values of time to peak seem to be poorly influenced by tanβ.

As a conclusion this analysis highlighted that the breach morphology is particularly important for dam breach events that happen in small (i.e. fast draining) reservoirs.

REFERENCES

Coleman, S. E., and Andrews, D. P. 2000. Overtopping breaching of noncohesive homogeneous embankment. *School of Engineering Report*, *Ref. no. 589*, Auckland, The University of Auckland, 368 pp.

Hanson G. J., Cook K. R. Hunt S. L. 2005. Physical modeling of overtopping erosion and breach formation of cohesive embankments. *Transaction of the ASAE (Am. Soc. of Agricultural Engineers)*, 48(5), 1783-1794.

Hunt S. L., Hanson G. J. Cook K. R., Kadavy K. C. 2005. Breach widening observations from earthen embankment tests. *Transaction of the ASAE*, 48(3), 1115-1120.

Investigation of Extreme Flood Process and Uncertainty (IMPACT). 2005. *WP2 publications-Technical reports.* http://www.impact-project.net/wp2_technical.htm (May 2010).

Macchione, F. 1986. Sull'idrogramma di piena conseguente alla rottura di dighe in terra. *Memorie e studi (External Memorandum)*, Dip. di Difesa del Suolo, Univ. della Calabria, Cosenza, Italy, No. 139.

Macchione, F. 2008. Model for predicting floods due to earthen dam breaching. I: Formulation and evaluation. *J. Hydraul. Eng.*, 134(12),1688-1696.

Macchione, F., and Rino, A. 2008. Model for predicting floods due to earthen dam breaching. II: Comparison with other methods and predictive use. *J. Hydraul. Eng.*, 134(12), 1697-1707.

Morris M., Hanson G., Hassan M. 2008. Improving the accuracy of breach modeling: why are we not progressing faster?. *J. Flood Risk Manag.,* 1, 150-161.

Powledge, George R., D.C. Ralston, P. Miller, Y.H. Chen, P.E. Clopper, and D.M. Temple. 1989. Mechanics of Overflow Erosion on Embankments. II: Hydraulic and Design Considerations. *J. Hydraul. Eng.*, 115(8), 1056-1075.

Rozov, A. L. 2003. Modeling of washout of dams. *J. Hydraul. Res.*, 41(6), 565-577.

Singh, V. P. 1996. *Dam breach modeling technology*, Kluwer Academic, Norwell, Mass.